ISSN 1070-3284, Russian Journal of Coordination Chemistry, 2014, Vol. 40, No. 8, pp. 547–557. © Pleiades Publishing, Ltd., 2014.
Original Russian Text © S.I. Pechenyuk, A.N. Gosteva, 2014, published in Koordinatsionnaya Khimiya, 2014, Vol. 40, No. 8, pp. 476–486.

The Complexes $[Ni_a(Pn)_b]_x[Fe(CN)_6]_y$ (Pn = 1,3-Diaminopropane): Synthesis and Thermolysis

S. I. Pechenyuk* and A. N. Gosteva

Tananaev Institute of Rare Element and Mineral Chemistry and Technology, Kola Research Center, Russian Academy of Sciences, Apatity, Russia

**e-mail: pechenyuk@chemy.kolasc.net.ru*

Received December 25, 2013

Abstract—The complexes $[Ni(Pn)_2]_2[Fe(CN)_6] \cdot 3H_2O$ (**I**), $[Ni_3(Pn)_5][Fe(CN)_6]_2 \cdot 9H_2O$ (**II**), $[Ni_5(Pn)_9][Fe(CN)_6]_3 \cdot 9H_2O$ (**III**), and $[Ni(Pn)_2]_3[Fe(CN)_6]_2 \cdot 6H_2O$ (**IV**) (Pn = 1,3-diaminopropane) were obtained. Their thermolysis was studied in oxidative (air), reductive (hydrogen), and inert atmospheres (argon) in a temperature range from 20 to 1000°C. Solid and gaseous products of the thermolysis were identified. In air thermolysis, the carbon of the ligands is eliminated as CO and CO_2; the solid residues consist of nickel oxide, iron oxides, and the intermetallide Ni_3Fe. In hydrogen thermolysis, the ligands are eliminated partially unchanged and partially hydrogenated to ammonia and hydrocarbons. The solid residue at >550°C consists of bimetallic phases with a small carbon impurity. In argon thermolysis, the ligands are eliminated partially unchanged or as fragments of the Pn molecule. The solid residues produced by calcination contain a mixture of metal and oxide phases and 10 to 20% of the initial carbon content.

DOI: 10.1134/S1070328414080090

INTRODUCTION

In the last two decades, the synthesis of heterometallic molecular entities (HMEs) has been of growing interest [1]. These compounds show attractive properties and can potentially be used in catalysis, medicine, nanotechnology, and, specifically, as precursors to nanosized bimetallic powders. Multiple HMEs with various ligands have been made; among them, a group of 3D HMEs with the CN ligands is of greatest interest. The anions $[Fe(CN)_6]^{3(4)-}$ are often used as the anion of these HMEs, and such HMEs are analogs of Prussian blue [2, 3]. A number of combinations of 3*d* metals have been investigated [1], including a few papers concerned with the combination Ni + Fe [4–7]. The air and hydrogen thermolysis of $[Ni(NH_3)_6]_3[Fe(CN)_6]_2$ has been reported only [7]. This complex decomposes in air by eliminating two NH_3 molecules at 60–190°C and the rest of ammonia at 190–250°C, leaving at 400°C a solid residue ($3NiO + Fe_2O_3$). During hydrogen thermolysis, this complex also loses ammonia stepwise. The N and C atoms of the cyano groups are eliminated as ammonia and hydrocarbons (mainly, methane). The solid residue consists of the intermetallide $Ni_{0.6}Fe_{0.4}$; however, this product even at 700°C contains 1/6 and 1/4 parts of the initial carbon and nitrogen contents, respectively. Therefore, the temperature required to remove all the ligands from this complex in a hydrogen atmosphere is appreciably higher than that in air. The thermolysis of the cationic and anionic complexes making up $[Ni(NH_3)_6]_3[Fe(CN)_6]_2$ involves a wider temperature range and follows a more complicated decomposition pattern [8, 9] via the simple salts $NiCl_2$ (for the cation) and $KCN + Fe(CN)_2$ (for the anion) as intermediate products.

The goal of the present work was to study the synthesis and thermolysis of the complexes $[Ni(Pn)_2]_2[Fe(CN)_6] \cdot 3H_2O$ (**I**), $[Ni_3(Pn)_5][Fe(CN)_6]_2 \cdot 9H_2O$ (**II**), $[Ni_5(Pn)_9][Fe(CN)_6]_3 \cdot 9H_2O$ (**III**), and $[Ni(Pn)_2]_3[Fe(CN)_6]_2 \cdot 6H_2O$ (**IV**) (Pn = 1,3-diaminopropane). The literature data for the thermolysis of these complexes and for the synthesis of complexes **I**, **II**, and **IV** are lacking. Complex **III** was obtained as described in [5]. The same but somewhat modified procedure was used for the synthesis of complexes **II** and **IV**. All the complexes under discussion seem to have complicated 2D and 3D structures. Their properties as well as air, hydrogen, and argon thermolysis were studied; the solid and gaseous products of the thermolysis were identified.

EXPERIMENTAL

The following starting materials were used: $NiCl_2 \cdot 6H_2O$ (reagent grade), $K_3[Fe(CN)_6]$, $K_4[Fe(CN)_6] \cdot 3H_2O$ (reagent grade), and 1,3-diaminopropane (Pn) (0.889 g/cm^3, Vekton). For the synthesis of HMEs, $[Ni(Pn)_2]Cl_2 \cdot 2H_2O$ was prepared as described in [10].

Synthesis of complex I. A weighed sample of $[Ni(Pn)_2]Cl_2 \cdot 2H_2O$ (1.55 g, 5 mmol) was dissolved in 82% ethanol (7 mL) and water (7 mL) to give a bright violet solution. Then $K_4[Fe(CN)_6] \cdot 3H_2O$ (2 mmol) as a 0.5 M solution (4 mL) and water (15 mL) were

added. This immediately resulted in the formation of a violet curdy precipitate. The reaction mixture was cooled to ~0°C for 1 h. The precipitate was filtered off, washed with ethanol, and dried in air. The yield of complex **I** was 1.25 g (~85%), anisotropic violet tabular crystals; the refractive indices are $N_p' = 1.623$, $N_g' = 1.644$.

For $C_{18}H_{52}N_{14}O_6Ni_2Fe$ (**I**)

anal. calcd., %:	C, 29.46;	Ni, 16.01;	Fe, 7.61.
Found, %:	C, 29.25;	Ni, 16.08;	Fe, 7.25.

Synthesis of complex II. A weighed sample of $NiCl_2 \cdot 6H_2O$ (14.4 g, 0.06 mol) was dissolved in ethanol (65 mL), and a mixture of Pn (15 mL, 0.18 mol) and water (75 mL) was added. Addition of $K_3[Fe(CN)_6]$ (13.16 g, 0.04 mol) to the resulting solution immediately produced a bronze-colored precipitate. The reaction mixture was cooled to ~0°C for 1 h. The precipitate was filtered off, washed with ethanol, and dried in air. The yield of complex **II** was 22.33 g (62.8%), anisotropic laminated crystals ranging in color from light yellow to red-brown with $N = 1.590–1.606$.

For $C_{27}H_{62}N_{22}O_6Ni_3Fe_2$ (**II**)

anal. calcd., %:	C, 30.03;	Ni, 16.34;	Fe, 10.35.
Found, %:	C, 30.24;	Ni, 16.11;	Fe, 10.05.

Synthesis of complex III [5]. A weighed sample of $NiCl_2 \cdot 6H_2O$ (9.52 g, 70 mmol) was dissolved in water (100 mL), and a mixture of Pn (10 mL, 120 mmol) and water (25 mL) was added. The resulting dark blue solution was stirred, and $K_3[Fe(CN)_6]$ (26.32 g, 80 mmol) in water (200 mL) was added for 5 min. This immediately resulted in the formation of a golden-brown precipitate. The reaction mixture was left for 24 h. The precipitate was centrifuged, suspended in water with subsequent centrifugation (4 times), washed with ethanol, and dried in air. The centrifugation was employed because of the poor filterability of the precipitate consisting of thin tabular crystals. The yield of complex **III** was 12.86 g (91.49%), anisotropic laminated crystals ranging in color from light yellow to red-brown with $N = 1.590–1.606$.

For $C_{45}H_{108}N_{36}O_9Ni_5Fe_3$ (**III**)

anal. calcd., %:	C, 30.73;	Ni, 16.70;	Fe, 9.53.
Found, %:	C, 0.78;	Ni, 16.61;	Fe, 9.74.

Synthesis of complex IV. A weighed sample of $[Ni(Pn)_2]Cl_2 \cdot 2H_2O$ (16.23 g, 52 mmol) was dissolved in ethanol (63 mL) and water (63 mL) to give a bright violet solution. Then $K_3[Fe(CN)_6]$ (9.18 g, 27.9 mmol) in water (140 mL) was added. The reaction mixture was cooled to ~0°C for 1 h. The brown precipitate that formed was filtered off, washed with ethanol, and dried in air. The yield of complex **IV** was 15.84 g (~98.67%), yellow anisotropic tabular formations. The pleochroism is yellow in N_p and olive-colored in N_g; $N_p' = 1.598$, $N_g' = 1.609$.

For $C_{30}H_{72}N_{24}O_6Ni_3Fe_2$ (**IV**)

anal. calcd., %:	C, 31.26;	Ni, 15.29;	Fe, 9.69.
Found, %:	C, 31.36;	Ni, 15.38;	Fe, 9.63.

The elemental analysis data were averaged over several measurements for different syntheses of the same complex; the standard deviations fell within 0.5%.

The complexes obtained were identified using elemental analysis, X-ray powder diffraction, IR spectroscopy, and crystal optics analysis. Analysis for metals was performed as follows. Weighed samples of the complexes and their thermolysis products were calcined at 700°C for 1.5 h to remove and then dissolved in dilute H_2SO_4. The resulting solutions were analyzed by atomic absorption spectroscopy on an AAnalyst 400 spectrometer. Analysis for carbon was carried out by automated coulometric titration on a CS-2000 express analyzer; the nitrogen and hydrogen contents were determined on a EURO EA-3000 instrument. X-ray powder diffraction was measured on DRON-2 and DRF-2 diffractometers (CuK_α radiation, graphite monochromator). IR spectra were recorded on a Nicolet 6700 FTIR spectrometer (in KBr pellets). The complexes were identified by comparing their spectra with the literature data [5, 9, 11–13]. Crystal optics was studied with a Leica DM 2500 microscope using a standard set of immersion fluids. The densities of the complexes **I–IV** were measured with a pycnometer in acetone at 25°C: $\rho = 1.558$ (**I**), 1.565 (**II**), 1.452 (**III**), and 1.523 g/cm^3 (**IV**).

The most intense reflections for complexes **I–IV** include (interplanar spacings d/n, nm)/I: 0.74/100, 0.50/80, 0.43/61, 0.40/69, 0.37/56, 0.31/48, 0.29/39, 0.28/64, 0.24/57 (**I**); 1.09/88, 0.80/63, 0.69/100, 0.60/88, 0.50/96, 0.46/83, 0.41/48, 0.37/56, 0.28/40 (**II**); 1.04/100, 0.78/33, 0.69/60, 0.66/70, 0.57/56, 0.54/62, 0.47/65, 0.45/69, 0.40/37, 0.37/44, 0.28/28 (**III**); 1.08/26, 0.96/18, 0.80/21, 0.69/43, 0.6/42, 0.50/100, 0.46/47, 0.38/21, 0.37/24 (**IV**).

The IR spectrum of complex **I** differs from those of complexes **II–IV**, featuring the following absorption bands (cm^{-1}): 3569 ν(OH); 3395 ν(OH, H_2O); 3323, 3272, 3173 ν(NH); 2885 ν(CH); 2053, 2037 ν(C≡N for Fe(II)). The IR spectra of complexes **II–IV** are in good agreement with each other (cm^{-1}): 3424, 3451, 3332 ν(OH_2); 3315, 3267–3272 ν(NH); 2933, 2885 ν(CH); 2110 ν(C≡N for Fe(III)).

Multiple absorption bands at 1600–500 cm^{-1} cannot be assigned unambiguously; however, they are all known to relate to inner-sphere propylenediamine [11]. In the IR spectra of complexes **II–IV**, these

bands coincide as well. In addition, their IR spectra show not only the ν(CN) bands due to the anion $[Fe(CN)_6]^{3-}$ (2110 cm^{-1}) but also weaker bands characteristics of the anions $[Fe(CN)_6]^{4-}$ (2053, 2037 cm^{-1}). The IR spectra suggest the similarity of these complexes, which is, however, not confirmed by data from elemental analysis, X-ray powder diffraction, and thermal analysis.

Thermal analysis was carried out on a Netzsch STA 409 PC/PG synchronous thermal analyzer by passing air and argon at a flow rate of 20 mL/min. A weighed sample (9–11 mg) was placed in a corundum crucible, exposed to a gas flow for 1 h, and heated at a rate of 10°C/min from 25 to 1000°C. The air and argon thermolysis of complexes **I–IV** was also studied with a MAG flow gas analyzer (OOO Monitoring, Russia). The instrument is designed to determine CO, CO_2, and organic materials converted to methane in the gas phase. A weighed sample (~0.2 g) was placed in a quartz boat, which was transferred to a flow quartz reaction tube placed in a SNOL-0.2/1250 tube furnace. The furnace was heated at a rate of 5°C/min; the gas flow rate was 1 L/min. The areas of the curves recorded in coordinates c (mol/L)–V(L) were used to determine the yields of the components of the gas flow as the percentages of the total carbon content. The areas of the curves were calculated with the MATHCAD-15 program.

We also examined the products corresponding to separate points on the DTA and DTG curves (cut-off). Weighed samples of the complexes were calcined in air at fixed temperatures in a SNOL 7.2/1100 muffle furnace. Hydrogen thermolysis of the complexes was carried out on a flow setup manufactured as described in [14] (a quartz tube placed in a SNOL 0.2/1250 electric tube furnace). The time of exposure proper to the temperatures above 200°C was 1 h (the time required to attain this temperature level is ignored). In all the experiments, the heating rate was 10°C/min; the flow rate of hydrogen and argon was 10–15 L/h. A GVCh-12K generator was used as a hydrogen source. Before use, bottle argon was passed through an alkaline suspension of $Mn(OH)_2$ to remove an impurity of O_2 and then dried by passing through concentrated H_2SO_4. Thermolysis products were cooled under H_2 or Ar. Solid reduction products were identified by X-ray powder diffraction using the database [13]; all the thermolysis products were analyzed for metal and carbon. Gaseous products were trapped in two Dreschel bottles connected in series. The first one contained 1 M HCl, and the second, 1 M NaOH. Analysis of the second adsorbing solution revealed the absence of acidic products. Fixed temperatures for the study of the thermolysis products were chosen so as to correspond to the midpoints of the temperature ranges for the most distinct decomposition steps. For hydrogen thermolysis, the temperatures were higher by ~50°C than those in air thermolysis because the complexes of Row I transition metals decompose in the presence of hydrogen at higher temperatures than they do in air [7]. Ammonia was identified among the gaseous thermolysis products, as in the thermal reduction of other HMEs containing the anions $[Fe(CN)_6]^{3(4)-}$ [7, 15]. High-boiling organic substances evolved as well; they condensed at the cold outlet of the reaction tube and in a special condenser provided before the gas analyzer. The IR spectra of these compounds contain absorption bands at 3000–2800 (CH stretches), 1700–1500 (NH_2 bends), and 1460–1360 cm^{-1} (CH_2 bends) [11], which is characteristic of Pn and products of its thermal degradation. Averaged empirical formulas of solid thermolysis products were calculated from the elemental analysis data for solid and gaseous products with powder diffraction data taken into account.

Thermal analysis in combination with evolved gas analysis by mass spectrometry (EGA-MS) today becomes increasingly popular. We employed EGA-MS in the study of the air and argon thermolysis of complexes **I** and **II**[1] on an Aeolos QMS 403 mass spectrometer coupled with a synchronous thermal analyzer for a mass number range of 10–80 Da. Products with 17, 18, 44 and 57 Da were detected. The results obtained are summarized in Tables 1–5 and shown in Figs. 1 and 2.

RESULTS AND DISCUSSION

Complex **I** is very different from complexes **II–IV**. The latter show close analyses for metal and carbon and very similar IR spectra. Distinctions between them emerge only from their X-ray powder diffraction patterns and thermal analysis data. Unfortunately, we failed to grow single crystals suitable for X-ray diffraction. Structures **I–IV** were determined from previous data for complex **III** [5]. However, when exactly following the procedure described in [5], we obtained a complex containing nine rather than ten Pn molecules and six rather than ten water molecules. According to X-ray diffraction data for $[Ni^{II}(Pn)_2]_5[Fe^{III}(CN)_6]_2[Fe^{II}(CN)_6] \cdot 10H_2O$ [5], all the cyano groups of $[Fe(CN)_6]^{4-}$ and two cyano groups of $[Fe(CN)_6]^{3-}$ are coordinated to the adjacent Ni ions. The asymmetric structural unit contains five *trans*-$[Ni^{II}(Pn)_2]^{2+}$ cations, two $[Fe(CN)_6]^{3-}$ anions, a $[Fe(CN)_6]^{4-}$ anion, and ten water molecules. The $[Fe(CN)_6]^{3-}$ anion is linked with two cations and the $[Fe(CN)_6]^{4-}$ anion is linked with six cations to form a 3D framework containing the fragments Fe(III)–CN–Ni(II) and Fe(II)–CN–Ni(II). The complex nickel cation is an oblate octahedron with a tetragonal distortion, which is made up of four N atoms of the amino ligand and two N atoms of the cyano groups. The Fe(III) anion has a nearly perfect octahedral geometry.

[1] We are grateful to I.V. Krivtsov (South Ural State University).

Table 1. Air thermolysis of complexes **I–IV**

C	Step	TG data, °C*			Weight loss, %	Residue, %	Empirical formula of the residue (at T, °C)	Phases present
		T_{lb}	T_{ub}	T_m				
I	1	40	100	130	4.1	95.9	$[Ni_2(C_3N_2H_{10})_4][Fe(CN)_6] \cdot 4H_2O$ (90)	Original
	2	130	170	190	6.8	89.1		
	3	190	205	270	15.7	73.4	$[Ni_2(C_3N_2H_{10})_3][Fe(CN)_6]$ (200)	XA**
	4	270	310	335	7.0	66.4		
	5	335	400	465	34.2	32.2	$Ni_2FeO_{2.6}$ (440)	Ni_3Fe, $NiFe_2O_4$
II	1	45	128	190	9.0	91.0	$[Ni_3(C_3N_2H_{10})_4CNH_4][Fe(CN)_6]_2 \cdot 3H_2O$ (105)	Original
	2	190	210	270	14.5	76.5	$[Ni_3(C_3N_2H_{10})_3C_{1.5}NH_5][Fe(CN)_6]_2$ (200)	XA
	3	270	310	335	7.8	68.7	$Ni_3Fe_2C_{0.1}O_{5.75}$ (320)	Ni, $Ni_{1.43}Fe_{1.7}O_4$
	4	335	390	415	18.1	50.6		
	5	415	435	490	16.0	34.6	$Ni_3Fe_2O_4$ (500)	Ni, NiO, Fe_2O_3, Fe_3O_4
III	1	40	80	160	6.6	93.4	$[Ni_5(C_3N_2H_{10})_9][Fe(CN)_6]_3 \cdot H_2O$ (125)	XA
	2	160	175	190	2.5	90.9		
	3	190	205	263	14.6	76.3		
	4	263	303	320	8.2	68.1	$Ni_5Fe_3C_{1.1}O_{10.3}$ (320)	Ni_3Fe, $NiFe_2O_4$
	5	320	420	470	34.1	34.0		
IV	1	25	125	175	7.7	92.3	$[Ni_3(C_3N_2H_{10})_5C_2NH_6][Fe(CN)_6]_2 \cdot 2.5H_2O$ (120)	XA
	2	175	210	265	15.7	76.6		
	3	265	305	340	7.8	68.8	$Ni_3Fe_2C_{1.8}N_3O_6$ (320)	NiO, $NiFe_2O_4$, Fe_3O_4
	4	340	400	415	15.1	53.7		
	5	415	430	475	13.5	40.2		
	6	475	495	520	5.9	34.3		

* T_{lb} and T_{ub} are the lower and upper bounds of the temperature range, respectively; T_m is the temperature within this range at which the weight loss is maximum.

** X-ray amorphous.

One can assume that structures **I**, **II**, and **IV** are similar to structure **III** since two cyano groups of adjacent Fe atoms can also be involved in coordination. However, it is not improbable that the resulting "islet" crystal structure is made up of the discrete, slightly distorted square cations $[Ni^{II}(Pn)_2]^{2+}$ and the octahedral anions $[Fe(CN)_6]^{4-}$ (**I**) and $[Fe(CN)_6]^{3-}$ (**IV**). Apparently, the ligands from the "islet" structures **I** and **IV** should be removed more easily than those from 3D structures. The bridging Pn molecule, which seems to be present in complex **II**, links two of three Ni atoms and hence already gives rise to a 3D structure, not to mention the formation of the bridges Fe(III)–CN–Ni(II).

Thermolysis in air. The TGA data for complexes **I–IV** subjected to air thermolysis are summarized in Table 1. Data for the products of the air thermolysis at fixed temperatures are given in Table 2. Complexes **I** and **II** do not lose all the water of crystallization below 130°C, retaining their original crystal structures. In contrast, complexes **III** and **IV** do not retain theirs. The solid residues produced by low-temperature calcination are virtually identical according to TG and cut-off data. The higher the temperature, the larger the weight difference between the residues. Clearly, at a constant heating rate of 10°C, the weight of the residue is not the same as that achieved when the complex is kept at a constant temperature for an hour.

In the thermolysis of HMEs, the anions $[Fe(CN)_6]^{3(4)-}$ begin to decompose at 350°C [9, 16]. Apparently, they retain intact below this temperature. That is why the decrease in the carbon content is due to removal (and due to combustion in air thermolysis) of the organic ligands from the cation. This allowed calculating the contents of elements in the residues.

When dried at 90°C, complex **I** retains its initial composition and four water molecules (Tables 1, 2); heating to 200°C results in elimination of a mole of Pn. Calcination of complex **I** at 450°C produces a residue with a weight (32.27%) close to $2NiO + 1/2Fe_2O_3$ (calculated: 31.26%). At 1000°C, the residue (30.33%) is close to $2NiO + 1/3Fe_3O_4$ (calculated: 30.90%). When this complex is kept at 450°C for 1 h, the residue contains less oxygen and the metallic phase

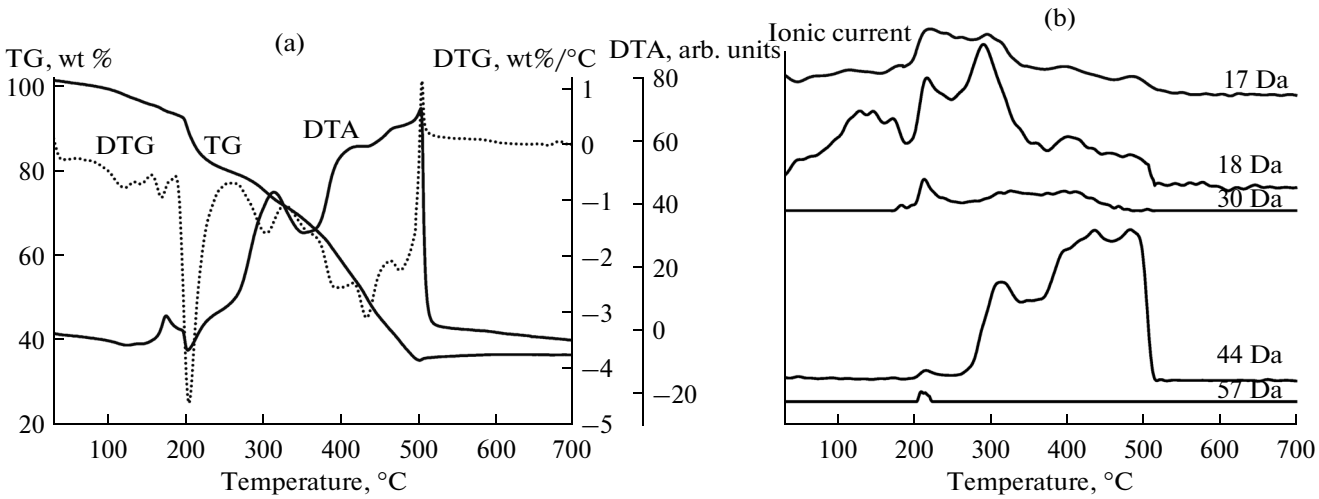

Fig. 1. (a) TG, DTG, and DTA curves and (b) MS data for complex **I** subjected to air thermolysis.

Ni_3Fe (Table 2). Complex **II** loses Pn (~2/3 mole) even at 105°C, although the residue still contains three of out six molecules of crystallization water. The original crystalline phase dominates. At 200°C, the residue contains only 3.5 moles of Pn and probably an impurity of finely divided oxides. At >300°C, the residue is a metal–oxide mixture (Table 2). The thermolysis of complex **II** is completed at 490°C; the residue (35.31%) remains unchanged up to 1000°C and corresponds to $3NiO + Fe_2O_3$ with a small impurity of magnetite. According to gas analysis data, all the carbon of complex **I** is removed at 310–360°C as CO (20%) and CO_2 (75%). The carbon of complex **II** is eliminated at 320–420°C mostly as CO_2 (95%). When kept at 320°C for 1 h, complex **II** loses almost all its carbon; under the same conditions, complexes **III** and **IV** still contain one and two C atoms, respectively.

Complex **III** at 125°C retains all its carbon and a water molecule, though becoming X-ray amorphous. Above 470°C, the weight loss is virtually not observed. The residue (34%) corresponds to $5NiO + Fe_3O_4$ (calculated: 34.43%). As with complexes **I** and **II**, the residue produced by exposure of complex **III** to a temperature of 320°C contains a metal phase (nickel) (Table 2). Complex **III** experiences the greatest weight loss at 320–470°C; for complex **IV**, this range is 415–575°C (the carbon in **IV** is harder to remove). Both complexes **III** and **IV** lose >95% of their carbon upon the 1-h exposure to 320°C. Complex **IV** loses much carbon as CO (22%), in contrast to complexes **II** and **III** (6 and 4%, respectively) (Table 3). The degradation of complex **IV** starts at 120°C. The weight of its residue (34.3%) remains constant above 520°C, being close to $3NiO + Fe_2O_3$ (33.3%) (Tables 1, 2).

X-ray powder diffraction revealed that the residues of calcined complexes **I–III** contain, along with oxide phases, the metal phases Ni and Ni_3Fe, which has never been noted for other HMEs [7, 17–19].

EGA-MS measurements during the air thermolysis of complexes **I** and **II** give virtually the same results (Fig. 1). One can see three temperature ranges of water (18 Da) elimination. Obviously, it is the water of crystallization that is eliminated below 200°C. At higher temperatures, water is produced by Pn oxidation. The latter process also gives ammonia eliminated together with water. Small amounts of products with 30 and 57 Da are detected in the same temperature range. They may be NO and $NH_2C_3H_5$ produced by Pn degradation. Combustion of carbon to CO_2 occurs below 500–550°C (clearly, this is the carbon of the cyano groups that is removed). Since the thermolysis of complexes **I** and **II** yields identical gases, we did not use EGA-MS for complexes **III** and **IV**.

Thermolysis in an argon atmosphere. The thermal analysis data for complexes **I–IV** subjected to argon thermolysis are summarized in Table 3. Data for the products of the argon thermolysis at fixed temperatures are given in Table 4. For all the complexes, the thermolysis occurs in a wider temperature range compared to air thermolysis. The weight losses occur up to 1000°C; the residues of the complexes calcined at this temperature contain 10–20% of the initial carbon content. EGA reveals no CO_2 among gases produced by the thermolysis of complexes **I–IV** under these conditions. Partial elimination of CO (1–2% C) is observed. Considerable amounts of Pn and its degradation products (in total, up to ~35–40% of the initial carbon content) are detected. Apparently, this value roughly corresponds to the amount of Pn condensed in connecting hoses. The initial steps (below ~200°C) of the air and argon thermolysis virtually coincide in temperature and result in nearly equal weight losses. Up to 30% of the initial nitrogen content is eliminated as ammonia. At close temperatures (>200°C), the residues of the complexes calcined under argon are always heavier than those in air. Calcination at 500–

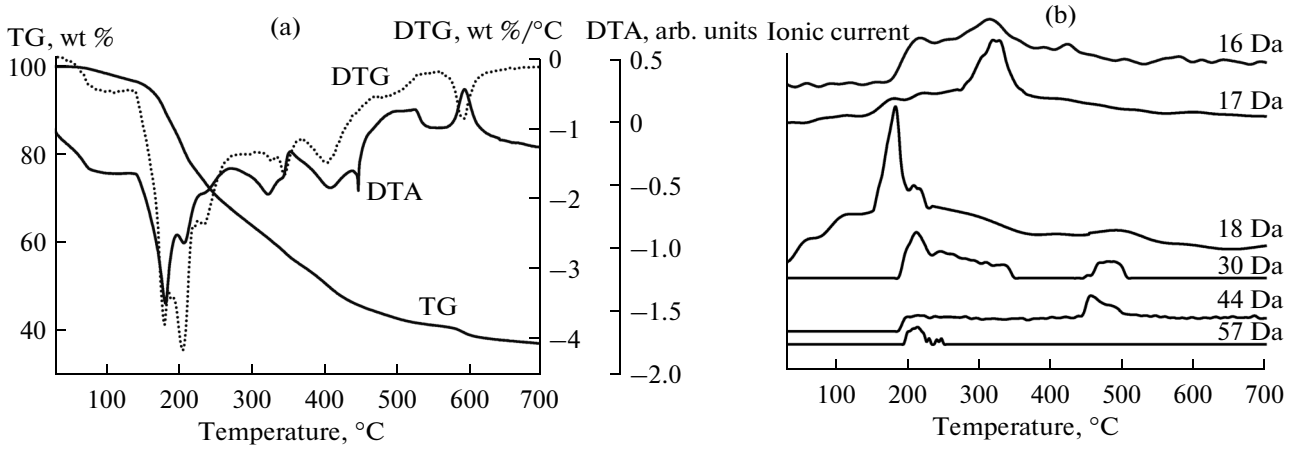

Fig. 2. (a) TG, DTG, and DTA curves and (b) MS data for complex **I** subjected to argon thermolysis.

600°C produces residues containing ~20% of the initial carbon content; at 1000°C, the residual carbon content is ~10% (Table 4).

According to X-ray powder diffraction data, the residue obtained by calcination at >350°C contains the phase Ni_3Fe and nickel carbides, nitrides, and hydrides, with impurities of oxides of both metals. Elemental analysis reveals the presence of considerable carbon impurities (15–20%) (Table 4); i.e., this is a strongly metalated mixture of many phases. The number of the O atoms in the empirical formulas suggests that oxides account for 15 to 50% of the metal in the residues; the highest oxide content is in the residue of complex **IV**. X-ray powder diffraction at the products of the argon or hydrogen thermolysis never produces a pattern containing a strong line at 3.36 Å due to graphite. Weak lines appear at 3.40, 3.41, and 3.45 Å in the diffraction patterns obtained upon the argon thermolysis of complexes **I** and **II** at >700°C. Therefore, the carbon impurity is an X-ray amorphous phase.

According to the EGA-MS data (Fig. 2), the argon thermolysis also produces gaseous products with 17, 18, 30, 44 and 57 Da. The first two products (17 and 18 Da) are ammonia and water, as in the air thermolysis. Water (apparently, the water of crystallization) is eliminated below 200°C. Ammonia is eliminated at 280–380°C as a result of Pn degradation. The product with 57 Da is eliminated at 200–250°C. The products with 30 and 44 Da are most likely not the same as in the oxidative atmosphere; they may be ethane and propane, respectively.

Based on the data obtained, we can propose the following sequence of transformations for the argon thermolysis of complexes **I–IV**. Below 200°C, the complexes lose most of their water and some of their coordinated Pn, as observed in air thermolysis. At higher temperatures, the elimination of Pn continues, with its further degradation into amino groups and other fragments. The oxygen of the remaining water is partially contained in the oxide phase and partially eliminated as CO. The residual carbon is partially contained in carbides and partially forms a separate amorphous phase, which seems to interleave oxide and metal particles.

Thermolysis in a hydrogen atmosphere. Data for the products of the thermal reduction of complexes **I–IV** are given in Table 5. In hydrogen thermolysis, complex **I** at 200°C loses 28% of its carbon, yielding $[Ni_2(C_3N_2H_{10})_2CNH][Fe(CN)_6] \cdot H_2O$. This formula is virtually the same as found for the air and argon thermolysis at this temperature. About two Pn molecules are sublimed to condense at the cold outlet of the reaction tube. At 440°C, 4.6% of the carbon is present in the solid state. The solid phase also contains the nickel metal and a solid solution of Ni_3Fe (X-ray powder diffraction data). At 670°C, the carbon content of the solid phase is nearly zero. Up to 1/3 of the nitrogen is eliminated as NH_3, which corresponds to the hydrogenation of ~4.5 out of six CN groups. Complex **II** behaves in a similar way, yielding at 200°C $[Ni_3(C_3N_2H_{10})_4C_{2.5}H_7][Fe(CN)_6]_2 \cdot 2.5H_2O$. This formula is close to that found for the air and argon thermolysis. The nitrogen is eliminated as NH_3, which corresponds to the hydrogenation of nine out of twelve CN groups. At 550°C, the residue of complex **II** contains no carbon. Apparently, a Fe-Ni solid solution cannot retain carbon in thermal reduction.

The residue of complex **III** reduced at 550°C contains 6.5% of its initial carbon content; for complex **IV**, the residual carbon content under the same conditions is 0.4%. In both cases, 45% of their nitrogen is eliminated as NH_3, which corresponds to the nearly complete hydrogenation of the cyano groups (16 out of 18 and 11 out of 12, respectively). Much of Pn is eliminated intact. By the residual carbon content upon the hydrogen thermolysis under static conditions, the complexes under discussion can be arranged as follows: **III** > **IV** > **I** ≈ **II**.

To sum up, despite the similarity of their physicochemical characteristics, complexes **I–IV** are individ-

Table 2. Products of the air thermolysis of the Ni–Fe complexes

Empirical formula/*M*	Thermolysis conditions (*T*, °C)	Residue, %		Phases present	Contents of the elements, %						
		exp.	calc.		Ni		Fe		C		
					exp.	calc.	exp.	calc.	exp.	calc.	% of the initial content
$C_{18}H_{52}N_{14}O_6Ni_2Fe$/733.24 (**I**)	Starting	100	100	Original	16.03	16.00	7.49	7.61	29.68	29.46	100
$C_{18}H_{48}N_{14}O_4Ni_2Fe$/701.24	90	95.8	95.6	Original	16.85	16.74	7.76	7.96	30.43	30.80	100
$C_{15}H_{30}N_{12}Ni_2Fe$/551	200	75.1	75.1	XA	20.98	21.29	9.92	10.13	32.49	32.65	83.33
$O_{2.6}Ni_2Fe$/216	440	29.7	29.7	Ni_3Fe, $NiFe_2O_4$	54.88	54.35	25.10	25.85	<0.03		<0.03
$C_{27}H_{62}N_{22}O_6Ni_3Fe_2$/1077.78 (**II**)	Starting	100	100	Original	16.11	16.34	10.30	10.35	30.24	30.03	100
$C_{25}H_{50}N_{21}O_3Ni_3Fe_2$/980	105	93.6	90.9	Original	17.95	17.97	10.39	11.39	30.66	30.62	92.69
$C_{22.5}H_{35}N_{19}O_2Ni_3Fe_2$/891	200	77.9	82.6	XA	19.95	19.78	11.88	12.55	30.67	30.34	83.33
$C_{0.1}O_{5.75}Ni_3Fe_2$/381	320	32.6	35.3	Ni, $Ni_{1.43}Fe_{1.7}O_4$	46.32	46.21	28.31	29.31	0.28	0.31	0.37
$O_4Ni_3Fe_2$/352	500	31.4	32.6	Ni, NiO, Fe_2O_3, Fe_3O_4	50.22	50.06	32.66	31.75	N/D	0	0
$C_{45}H_{108}N_{36}O_9Ni_5Fe_3$/1756.97 (**III**)	Starting	100	100	Original	16.61	16.70	9.74	9.53	30.78	30.73	100
$C_{45}H_{92}N_{36}ONi_5Fe_3$/1613	125	91.2	91.8	XA	17.11	18.20	10.32	10.39	33.20	33.50	100
$Ni_5Fe_3C_{1.1}O_{10.3}$/597	320	36.4	34.0	Ni_3Fe, $NiFe_2O_4$		49.13	27.19	28.05	2.06	2.06	2.28
$C_{30}H_{72}N_{24}O_6Ni_3Fe_2$/1151.75 (**IV**)	Starting	100	100	Original	15.38	15.29	9.63	9.69	31.36	31.26	100
$C_{29}H_{61}N_{23}O_{2.5}Ni_3Fe_2$/1059	120	91.5	91.2	XA	16.2	16.63	10.43	10.55	32.64	32.87	96.66
$C_{1.8}N_3O_6Ni_3Fe_2$/428	320	36.9	40.4	NiO, $NiFe_2O_4$, Fe_3O_4	39.17	41.12	25.00	26.08	4.75	5.04	5.99

* N/D—not detected.

Table 3. Argon thermolysis of complexes **I–IV**

Complex	Step	TG data, °C			Weight loss, %	Residue, %	Empirical formula of the residue (at T, °C)	Phases present
		T_{lb}	T_{ub}	T_m				
I	1	40	92–140	150	3.9	96.1		
	2	150	175	195	6.5	89.6		
	3	195	205	230	11.3	78.3	$[Ni_2(C_3N_2H_{10})_2CNH][Fe(CN)_6] \cdot 2H_2O$ (200)	XA
	4	230	235	290	11.8	66.5		
	5	290	360	445	14.8	51.7	$Ni_2FeC_{4.7}N_{5.7}$ (440)	Ni, Ni_3C, Ni_3N, Ni_2H
	6	445	505	550	13.3	38.4		
	7	550	570	665	14.4	24.0	Ni_2FeC_3NO (670)	Ni_3Fe, $NiFe_2O_4$, NiO, Fe_2O_3, Fe_3O_4
	8	665		1000	−6.6	30.6		
II	1	45	120	195	9.2	90.8		
	2	195	210	345	26.6	64.2	$[Ni_3(C_3N_2H_{10})_4C_2N_{1.5}H_4][Fe(CN)_6]_2 \cdot 2H_2O$ (200)	XA
	3	345	380	545	21.5	42.7		
	4	545	600	710	8.0	34.7	$Ni_3Fe_2C_{7.6}N_{5.5}O$ (550)	Ni_3Fe, $Ni_{1.43}Fe_{1.7}O_4$
	5	710	770	1000	6.5	28.2		
III	1	40	130	190	8.3	91.7		
	2	190	205	335	26.0	65.7		
	3	335	380	545	22.7	43.0	$Ni_5Fe_3C_{13}N_{13}O_3$ (550)	Ni_3Fe, Fe_3O_4
	4	545	610	1000	12.1	30.9		
IV	1	25	120	175	7.3	92.7		
	2	175	215	275	18.9	73.8		
	3	275	295	335	7.3	66.5		
	4	335	380	550	23.0	43.5	$Ni_3Fe_2C_{6.7}NO$ (550)	Ni, $NiFe_2O_4$
	5	550	615	750	9.6	33.9		
	6	750		1000	6.1	27.8		

Table 4. Products of the argon thermolysis of the Ni–Fe complexes

Empirical formula/*M*	Thermolysis conditions (*T*, °C)	Residue, %		Phases present	Contents of the elements, %							Nitrogen eliminated as NH_3, % of the initial content
		exp.	calc.		Ni		Fe		C			
					exp.	calc.	exp.	calc.	exp.	calc.	% of the initial content	
733.24 (**I**)	Starting complex	100	100	Original	16.03	16.00	7.49	7.61	29.68	29.46	100	
$C_{13}H_{25}N_{11}O_2Ni_2Fe/540$	200	77.6	73.7	XA	22.00	21.73	10.15	10.34	29.09	28.89	71.22	~6
$C_{4.7}N_{5.7}Ni_2Fe/309$	440	42.0	42.2	Ni, Ni_3C, Ni_3N, Ni_2H	37.63	37.94	17.98	18.04	18.24	18.23	25.60	~20
$C_3H_{0.8}N_{0.34}O_{1.5}Ni_2Fe/239$*	670	32.7	32.9	Ni_3Fe, $NiFe_2O_4$, NiO, Fe_2O_3, Fe_3O_4	48.96	49.11	23.68	23.36	14.90	15.06	16.67	~23.4
1077.78 (**II**)	Starting complex	100	100	Original	16.11	16.34	10.30	10.35	30.24	30.03	100	
$C_{26}H_{50}N_{21}O_2Ni_3Fe_2/976$	200	85.2	90.5	XA	17.94	18.04	11.24	11.44	32.15	31.97	96.30	~5.5
$C_{19}H_{28}N_{17}O_2Ni_3Fe_2/814$	300	69.8	75.5	XA	21.15	21.64	13.35	13.73	27.63	28.02	70.50	~6
$C_{15}H_{10}N_{14}O_{5.5}Ni_3Fe_2/762$	380	56.2	69.7	Ni_3Fe, Ni_3C, Ni_2H	23.30	23.11	14.68	14.65	23.12	23.62	55.60	~26
$C_{7.6}N_5ONi_3Fe_2/465$	550	39.2	43	Ni_3Fe, $Ni_{1.43}Fe_{1.7}O_4$	38.11	37.86	23.39	24.01	19.06	19.61	28.90	~25.3
1756.97 (**III**)	Starting complex	100	100	Original	16.61	16.70	9.74	9.53	30.78	30.73	100	
$C_{13}H_7N_4O_{6.6}Ni_5Fe_3/786$**	550	40.8	44.7	Ni_3Fe, Fe_3O_4		37.33	21.3	21.30	20.00	19.85	28.90	~29.3
$C_{5.6}O_3Ni_5Fe_3/576$	1000	32.2	32.8	NiO, Ni_3Fe, $NiFe_2O_4$, Fe_3O_4					11.81	11.63	12.40	~37
1151.75 (**IV**)	Starting complex	100	100	Original	15.38	15.29	9.63	9.69	31.36	31.26	100	
$C_7H_{3.3}N_{1.6}O_{4.5}Ni_3Fe_2/469$***	550	36.3	40.7	Ni, $NiFe_2O_4$	37.70	37.50	23.75	23.79	17.60	17.87	22.00	~31
$C_{2.7}O_3Ni_3Fe_2/368$	1000	31.1	31.9	NiO, Ni_3Fe, $NiFe_2O_4$, Fe_3O_4					8.87	8.80	9.00	~95

* Found (%): N, 2.00; H, 0.35. Calculated (%): N, 1.93; H, 0.33.
** Found (%): N, 6.85; H, 0.90. Calculated (%): N, 7.12; H, 0.89.
*** Found (%): N, 4.70; H, 0.70. Calculated (%): N, 4.77; H, 0.70.

Table 5. Products of the hydrogen thermolysis of the Ni–Fe complexes

Empirical formula/*M*	Thermolysis conditions (*T*, °C)	Residue, %		Phases present	ontents of the elements, %							Nitrogen eliminated as NH_3, % of the initial content
		exp.	calc.		Ni		Fe		C			
					exp.	calc.	exp.	calc.	exp.	calc.	% of the initial content	
733.24 (**I**)	Starting complex	100	100	Original	16.03	16.00	7.49	7.61	29.68	29.46	100	
$C_{13}H_{23}N_{11}ONi_2Fe$/522	200	76.6	71.2	XA	22.89	22.49	10.26	10.69	29.91	29.88	72.20	~3.5
$C_{0.7}NNi_2Fe$/196	440	26.7	26.7	Ni, Ni_3Fe	60.70	60.00	29.22	28.54	4.60	4.29	3.90	~30.6
$N_{0.6}Ni_2Fe$/182	670	24.8	24.8	Ni, Ni_3Fe	63.28	64.58	29.47	30.72	0.01		<0.01	~32.5
1077.78 (**II**)	Starting complex	100	100	Original	16.11	16.34	10.30	10.35	30.24	30.03	100	
$C_{26}H_{51}N_{20}O_{2.5}Ni_3Fe_2$/981*	200	84.1	87.3	XA	18.76	17.95	11.32	11.39	31.85	31.80	96.30	~6
$C_{1.5}Ni_3Fe_2$/306	380	27.6	28.4	Ni_3Fe	56.94	57.54	36.11	36.50	5.14	5.88	5.50	~34.2
Ni_3Fe_2/288	550	25.8	26.7	Ni_3Fe	61.52	61.18	38.48	38.83	N/D**	N/D**	N/D**	~39.2
1756.97 (**III**)	Starting complex	100	100	Original	16.61	16.70	9.74	9.53	30.78	30.73	100	
$C_3N_3Ni_5Fe_3$/539	550	28.5	30.67	Ni_3Fe	52.96	54.44	31.21	31.08	6.49	6.65	6.50	~44
1151.75 (**IV**)	Starting complex	100	100	Original	15.38	15.29	9.63	9.69	31.36	31.26	100	
$C_{0.12}N_{0.9}Ni_3Fe_2$/288	550	25.2	24.98	Ni_3Fe	58.32	58.32	37.04	36.99	0.488	0.487	0.40	~45

* Found (%): N, 28.20; H, 5.2. Calculated (%): N, 28.55; H, 5.2.
** N/D—not detected.

ual complexes with different structures. Complex **III** eliminates the carbon most reluctantly because of its 3D structure with bridging cyano groups [5]. The hydrogen thermolysis of complexes **I–IV** produces purely metal products. Below 200–250°C, these complexes behave in a similar way, regardless of their environment (air, argon, or hydrogen). The environment becomes crucial for their thermolysis at higher temperatures.

REFERENCES

1. Pechenyuk, S.I. and Domonov, D.P., *J. Struct. Chem.*, 2011, vol. 52, no. 2, p. 412.
2. Buser, H.J., Schwarzenbach, D., Petter, W., and Ludi, A., *Inorg. Chem.*, 1977, vol. 16, p. 2704.
3. Roy, X., Thompson, L.K., and Coombs, N., Maclachlan, M.J., *Angew. Chem., Int. Ed. Engl.*, 2008, vol. 47, p. 511.
4. Long Jiang, Hye Jin Choi, Tong Bu Lu, and Long, J.R., *Inorg. Chem.*, 2007, vol. 46, p. 2181.
5. Zhan Shu-zhong, Yu Kai-bei, and Liu Jiang *Inorg. Chem. Commun.*, 2006, vol. 9, p. 1007.
6. Pechenyuk, S.I., Semushina, Yu.P., Domonov, D.P., and Mikhailova, N.L., *Russ. J. Coord. Chem.*, 2006, vol. 32, no. 8, p. 572.
7. Domonov, D.P., *Cand. Sci. (Chem.) Dissertation*, Novosibirsk: Institute of Inorganic Chemistry, 2009.
8. Rejitha, K.S., Ishikawa, T., and Mathew, S., *J. Therm. Anal. Calorim.*, 2011, vol. 103, p. 515.
9. Mohai, B., *Z. Anorg. Allem. Chem.*, 1972, vol. 392, p. 287.
10. House, D.A., *J. Am. Chem. Soc.*, 1964, vol. 86, p. 223.
11. Nakamato, K., *Infrared and Raman Spectra of Inorganic and Coordination Compounds*, New York: Wiley, 1986.
12. *Thermoanalytical Curves*, Budapest: Acad. Kiado, 1976.
13. JCPDS-JCDD card. Newtown Square (PA, USA): International Centre for Diffraction Data, 2002.
14. Ginzburg, S.I., Gladyshevskaya, K.A., Ezerskaya, N.A., et al., *Rukovodstvo po khimicheskomu analizu platinovykh metallov i zolota* (Guide for Chemical Analysis of Platinum Metals and Gold), Moscow: Nauka, 1965.
15. Pechenyuk, S.I., Domonov, D.P., Avedisyan, A.A., and Ikorskii, S.V., *Russ. J. Inorg. Chem.*, 2010, vol. 55, no. 5, p. 734.
16. Ng, C.W., Ding, J., and Gan, L.M., *J. Solid State Chem.*, 2001, vol. 156, p. 400.
17. Pechenyuk, S.I., Domonov, D.P., Gosteva, A.N., et al., *Russ. J. Coord. Chem.*, 2012, vol. 38, no. 9, p. 596.
18. Pechenyuk, S.I., Gosteva, A.N., Domonov, D.P., and Makarova, T.I., *Vestnik Yuzhno Ural. Gos. Univ. Khimiya*, 2012, no. 24, p. 4.
19. Pechenyuk, S.I., Domonov, D.P., Gosteva, A.N., et al., *Izv. S.-Peterburg. Gos. Tekh. Inst. (Tekh. Univ.)*, 2012, vol. 15, no. 41, p. 18.

Translated by D. Tolkachev